

# Equilibria and Electronic Processes

A. M. STONEHAM\* AND MARTA M. D. RAMOS†‡

\*AEA Chief Scientist, 424-4 Harwell, Didcot, Oxford, OX11 0RA, United Kingdom;

†Department of Materials, University of Oxford, Oxford, United Kingdom

Received December 4, 1992; accepted December 23, 1992

IN HONOR OF SIR JOHN MEURIG THOMAS ON HIS 60TH BIRTHDAY

The operation of solid-state gas sensors and of certain types of catalyst depends on the energy of free carriers in one phase relative to some state in another medium. Here special problems arise in determining the electron affinity of ionic crystals. These are discussed, together with some of the issues which cause similar problems in different types of systems, here including aqueous solutions and conducting polymers. For ionic solids, knowledge of which charge states are stable for substitutional transition metal ions gives a powerful tool, giving predictions in accordance with electrochemical data. It appears that MgO has a negative electron affinity.

## 1. Introduction

In many circumstances there is a need to understand how electrons are distributed between different types of defects or between different media. Important examples are solid-state gas sensors and certain types of catalyst. In sensor operation, the mechanism exploits adsorption of some molecule, its possible reaction with another adsorbed species (like the molecular oxygen ion ( $O_2^-$ )), and transfer of a carrier into the substrate, thus affecting the electrical properties. In catalyst operation, one of the four main classes of mechanism is for the solid catalyst to provide an electron (or to act as an electron sink) in a critical step. The question we address concerns "free" carriers, those not localized at any specific defect: What energy should we assign to free electrons in the bulk of the solid when we wish to calculate the equilibria?

The question may seem trivial: "free" electrons in a solid are at the bottom of the

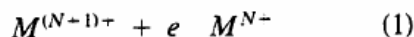
conduction band. Does the band picture not give us all we need? Let us ignore for the present two basic problems, namely the inadequacies of one-electron models (most people's idea of band theory (2)), and whether or not equilibrium is actually achieved in low-conductivity insulators. We must still ask where is the bottom of the conduction band in a form useful when we want to equilibrate two media, e.g., relative to an imaginary stationary electron at infinity? There are several twists to the tale. First, the interface between media can cause problems: a dipole layer at the interface will change the energy needed to take a charge across that interface (3-5). Second, we may wish to use the free carrier energy in an energy cycle in which some energies are calculated, and need to be combined with other data in a consistent way. Third, we may need to combine more than one theoretical model when we treat two very different types of media in contact (e.g., ionic solid and conducting polymer) and this requires particular care. There are no special difficulties other than band offsets when free carriers are delocalized and where defect

‡ Present address: Physics Department, University of the Minho, 4719 Braga, Portugal

energies are measurable relative to band energies (the traditional semiconductor situation); there are no major problems when carriers are localized (e.g., transition metal oxides, if both electrons and holes are small polarons). The cases which cause most difficulties are those where carriers are delocalized, and where, for good reasons, defect energies are not simply located relative to band edges. We shall use  $\text{MgO} : X$  ( $X$  being a transition metal ion) for much of our discussion, since there are extensive results from theory (6–8). Some of the analysis has been outlined before in an unpublished report (10).

## 2. Redox Energies in Ionic Solids

The main condition for charge transfer is one of energy. Exothermic reactions proceed; endothermic reactions occur only at a high enough temperature. For free atoms or molecules, the ionization potential  $I$  is sufficient to define the energy. For reasons which will become clear, we shall write  $I$  in the form  $I(N/N + 1)$ , meaning that the transition:



for the capture of an electron with zero kinetic energy at infinity (the so-called vacuum reference state) emits energy  $I(N/N + 1)$ . An electron with energy  $-I(N/N + 1)$  relative to the vacuum reference level (the  $-$  sign means below it) could combine with  $M^{(N+1)+}$  or be removed from  $M^{N+}$  with zero energy change. The redox potential in electrochemistry is very closely related. For a reaction like  $\text{Fe}^{2+} \rightarrow \text{Fe}^{3+} + e$ , with the electron state defined normally by a chosen half reaction, the standard expression for the redox potential is

$$\varepsilon - \varepsilon_0 = -(RT/F) \ln\{[\text{Fe}^{2+}]/[\text{Fe}^{3+}]\}, \quad (2)$$

If we choose  $e$  as a stationary electron at infinity, then  $\varepsilon - \varepsilon_0$  is just  $-I(2+/3+)$ .

The same concept occurs in the solid. However, there are four main types of cor-

rection. By far the largest correction is from polarization and distortion of the host lattice because of the altered local charge. Covalency needs careful definition (11), but there is no evidence for large covalent contributions to charge transfer energies in the ionic systems we discuss. Crystal field energies can usually be estimated to acceptable precision from optical spectra. The changes in total crystal field energy with charge state are often quite small. Finally, Jahn–Teller energies are small except in special cases which are easily identified.

The leading correction to  $-I(N/N + 1)$  is thus that from polarization and distortion. The correction can be estimated by methods originally due to Mott and Littleton (12), embodied in the Harwell HADES codes, and applied to related problems in (6). The result is an energy of the form (where the  $N + 1$  state is the more positive):

$$E(N + 1/N) = E(N/N + 1) \\ = w_{N+1} - w_N - I(N/N + 1), \quad (3)$$

which corresponds roughly to a Redox potential. Here  $w_N$  is the energy required to remove a host ion (e.g.  $\text{Mg}^{2+}$ ) and replace it by the impurity ion  $M$  in its  $N+$  charge state, all states being fully relaxed to equilibrium. An electron whose energy lies above  $E(N/N + 1)$  can be captured exothermically by  $M^{(N+1)+}$ ; an empty state below energy  $E(N/N + 1)$  will accept an electron from  $M^{N+}$ . In particular, stable states  $M^{N+}$  will correspond to  $E(N/N + 1)$  below the conduction band and  $E(N/N - 1)$  above the valence band (Fig. 1). These energies are not the one-electron energies of band theory, though they give rise to apparently very similar energy diagrams. However, they have a different meaning. In one-electron theory, stability means merely a level in the band gap, and  $E(N/N - 1)$  and  $E(N/N + 1)$  are presumed effectively equal. The Hubbard  $U$  parameter, which is a measure of electron-electron interaction is given by

$$U = E(N/N - 1) - E(N/N + 1) \quad (4)$$

in our notation.

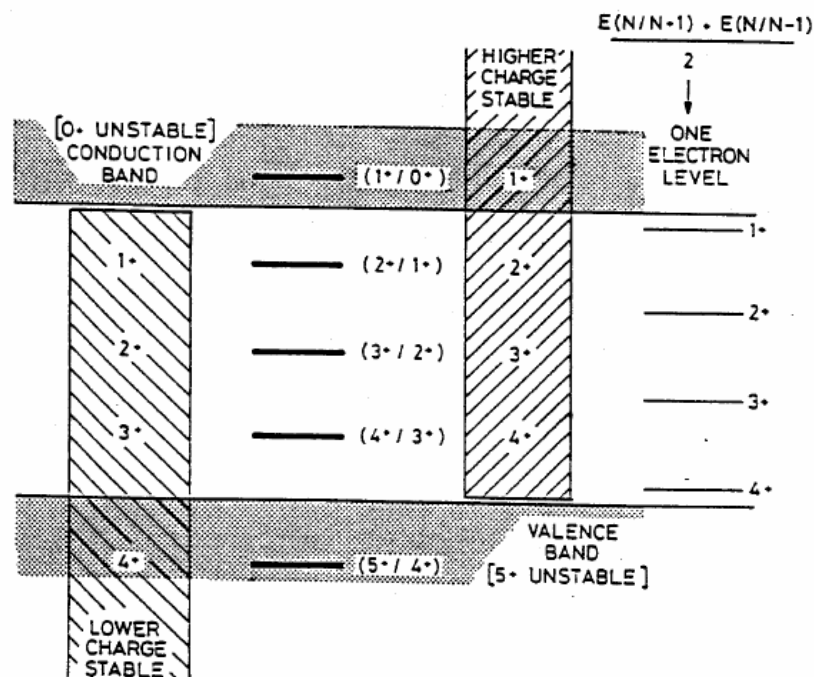


FIG. 1. Energetics and redox potentials for transition metal ions in MgO. These approximate results are based on Eqs. (3, 5) and use  $I(N/N + 1) = 16N$  eV,  $A = 24$  eV, and  $B = 6$  eV. More accurate values are given in Fig. 2.

### 3. Stability of Different Charge States in MgO

We now illustrate these ideas with data for transition metal ions in MgO. For clarity, we shall estimate energies in an oversimple way. The results we have given in our earlier work (6, 7) go substantially further, and it is these more accurate results which are used when specific predictions are given.

Charge state stability requires three main processes to be endothermic: the loss of an electron to the conduction band; the gain of an electron from the valence band; and charge disproportionation, in which one ion gains an electron from another. We now turn to the main energy terms involved.

#### 3.1. Ionization Energies

The broad trends in ionization energy for free ions (available from standard sources (13)) may be summarized thus. For the iron group (3d series),  $I(N/N + 1)$  is approxi-

mately  $16N$  eV for  $N = 1, 2, 3$ . For the rare earths (4f series),  $I(N/N + 1)$  is about  $22(N - 1)$  eV for  $N = 2, 3, 4$ . The variations from ion to ion within each series are modest but big enough to matter for any detailed study. For our purposes, the trends suffice. There is, of course, no need to assume free-ion data, for modern quantum chemistry approaches (e.g., the Harwell ICECAP code) can evaluate all the key energies. This has been done by (9), and confirms many of the points we make here.

#### 3.2. Ion Replacement Energies

These are the energies to remove a host ion and to replace it by the impurity in its chosen charge state, the host lattice being polarized and relaxed to equilibrium at each step. Values of these replacement energies  $w_N$  are best discussed in terms of the net charge  $Z$  (e.g., for  $\text{Fe}^{3+}$  ( $N = 3$ ) replacing  $\text{Mg}^{2+}$  ( $N = 2$ ) the net charge is  $3 - 2 =$

1). There are three main terms for a given species:

$$w_N = W_0 + AZ + BZ^2. \quad (5)$$

The difference contributing to  $E(N + 1/N)$  is given by:

$$-w_N + w_{N+1} = (A + B) + BZ \quad (6)$$

In Eq. (5)  $W_0$  is determined mainly by ion size, and is mainly an elastic energy. Term  $A$  comes from the Madelung energy, which depends on crystal structure. Term  $B$  comes from the polarization energy. In a simple cavity model we have

$$B \sim (e^2/2R)(1 - \epsilon_0^{-1}), \quad (7)$$

where  $R$  is not, in fact, the nearest neighbor distance (see later). For MgO,  $A \sim 24$  eV,  $B \sim 6$  eV, and it is easily seen that  $w_{N+1} - w_N$  can be tens of eV, i.e., a very large energy indeed.

We may use the same figures to estimate  $U$  (Eq. 4). Suppose an iron-group ion substitutes for a host cation of charge  $N_0$  (so  $N_0 = 2$  for MgO and  $N_0 = 4$  for  $\text{TiO}_2$ ). If we combine (6) with the expression for the ionization potential from Section 3.1:

$$E(N/N + 1) = [A + (1 - 2N_0)B] - [16 - 2B]N,$$

and  $U = [16 - 2B]$  eV, from Eq. 4. Thus  $U$  is usually positive and (with  $B \sim 6$  eV) around 4 eV, in agreement with (7), irrespective of many details of the oxide. For a rare-earth,  $U$  is larger, of order  $[22 - 2B]$  eV. As is obvious, the larger ionization potentials will reduce the number of stable charge states.

Is the value  $B \sim 6$  eV typical of other hosts too? The data for  $\text{TiO}_2$  of (14, 15) suggest that  $E(2+/3+)$  is near the conduction band edge for Cr and Fe, whereas  $E(3+/4+)$  is near the valence band edge. This would imply  $B \sim 6.4$  eV, a sensible value. However, V and Mn levels indicate this simple picture is rather too simple, though only modest ion-dependent terms in  $B$  would be necessary to make all consistent.

Full calculations by (16) suggest  $B \sim 6.1$  eV for the replacement of  $\text{Ti}^{4+}$  by  $\text{Ti}^{3+}$ .

We remark here the enormous differences in mechanism between ionic solids like MgO and semiconductors like the III-V's. In MgO covalency and charge transfer from an impurity to its oxygen neighbors is essentially negligible (and indeed this is confirmed in many ways, cf. (11)); it is Coulomb energies and polarization which dominate. For the III-V's (17) the dominant term is charge transfer through hybridization (indeed the number of electrons associated specifically with the transition metal changes very slowly with nominal charge state) and the Madelung terms are largely negligible. Despite these huge differences, as well as the differences in band gap, hosts like MgO and GaAs support typically three or even four charge states of most 3d transition metal ions (see (18, p. 255)).

### 3.3. Approximations for the Polarization Energy

If we had used Eq. (7) with nearest neighbor distance and static dielectric constant for MgO, we should have found  $B$  about 3 eV, roughly half the correct value. Since Eq. (7) is regarded as standard for complex systems, and for aqueous solutions, it is essential to realize its weakness and to understand the reasons. This can be done by revisiting the original work of Mott and Gurney (19, p. 60).

The general approach is the following. The crystal is divided into an inner region I, close to the defect, and a distant region II. In region II, dipole moments are calculated in terms of the electrical displacement due to the net charge of region I. In region I, the dipole moment  $\mu$  of any ion is induced by the sum of three contributions to the field which polarizes it: that due to other dipoles in the same shell of ions, that due to other dipoles and charges in region I, and that from region II. The field is itself linear in  $\mu$ , so one has to solve an equation of the sort

$$\mu = \alpha(a\mu + b). \quad (8)$$

It is simple to calculate the potential at the

central defect site due to the induced dipoles, which is directly related to the polarization term we calculate.

As a working approximation, we take the smallest possible region I, and we assume there are only two types of ion: type 2 (here cations), normally occupying the substitutional site at which the impurity occurs, and type 1 (here anions), the usual neighbor which is the species most strongly polarized. Carrying through the arguments gives  $R_{\text{eff}}$ , the effective cavity radius, in terms of  $a$ , the nearest neighbor distance. If we assign polarizabilities  $\alpha_1$ ,  $\alpha_2$  to the two host species, we obtain:

$$R_{\text{eff}}/a = (\alpha_1 + \alpha_2)/(\sigma_1\alpha_1 + \sigma_2\alpha_2), \quad (9)$$

where the  $\sigma_i = (\frac{1}{2}\pi) \sum_j (a/r_j)^4$  are sums over sublattices ( $i = 1, 2$ ); for the MgO structure  $\sigma_1 = 1.6230$  and  $\sigma_2 = 1.0082$ . For a defect on the cation site, we find these limiting cases:

Only anion polarizable (a reasonable approximation for MgO):  $R_{\text{eff}} = 0.616a$   
 Only cation polarizable:  $R_{\text{eff}} = 0.99a$   
 Equal anion and cation polarizabilities:  
 $R_{\text{eff}} = 0.76a$

We see  $R_{\text{eff}}$  is significantly smaller (and the polarization energy significantly larger) than the simple cavity model suggests. Presumably an extended region I would go over systematically towards the value  $R_{\text{eff}}/a \sim 0.5$  found from HADES calculations.

The results imply two rules. First, the common approximation given in Eq. (7) may be adequate when the impurity is placed on that sublattice which is itself especially polarizable. Second, Eq. (7) underestimates polarization energies badly when it is the nearest-neighbor sublattice which is highly polarizable. It is interesting that (20) found empirically that, for  $\text{TiO}_2 : \text{Mo}^{N+}$ , the charge states observed required a change in cavity radius (in effect, this was not the way he described it) to  $(3.7/6.0) = 0.62$  of the nearest neighbor distance, i.e., almost exactly the value from  $R_{\text{eff}}/a$  above, albeit for a crystal of different structure.

### 3.4. Comments on the Madelung Energy

For solid-state sensor applications, we may need to evaluate Eq. (3) for very complex crystal structures. It is therefore helpful to look at underlying trends. Here, there is guidance from some results due to Professor R. Pandey (given in (10)) for various charge states of Eu in the oxides of Mg, Ca, Sn, Ce, and U. What is striking is that the lattice contributions to  $E(N + 1/N)$  vary rather little from host to host. Even though the individual energy terms differ by tens of eV, the lattice terms in  $E(1/0)$  spread by only 3 eV and those for  $E(5/4)$  by just over 4 eV. Some of the insensitivity to structure comes from the relationship between coordination and interatomic distance (21), which means that the Madelung terms do not vary quite as much as expected. However, the compensation is not accurate enough for detailed assessment.

### 3.5. Dependence on Crystal Electron Affinity

If we compare the charges of stable species in MgO, CaO, and  $\text{SrTiO}_3$  (22), we see mainly a shift in their charge states. In both cases about the same number of stable states is obtained (i.e., three or perhaps four in cases like Fe) but spanning different actual charges. Thus for Ni in MgO, one sees the 1+, 2+, and 3+ states, and in  $\text{SrTiO}_3$  the 2+, 3+, and 4+ states. Similar results (albeit with gaps) occur throughout the iron group. This suggests (as Müller observes) that a large part of the difference stems from the electron affinity. In MgO a change of about 4 eV (namely from -1 eV to +2.5 eV) would change the stable charge state by one unit in the simplest model. Such a change would lead to essentially complete agreement with experiment (see Fig. 2). This change is roughly consistent with the extrapolation of some of the standard estimates of the differences between MgO and  $\text{SrTiO}_3$  from electrochemistry (23-25). These are based on some direct measurements of flat band potentials, a location of

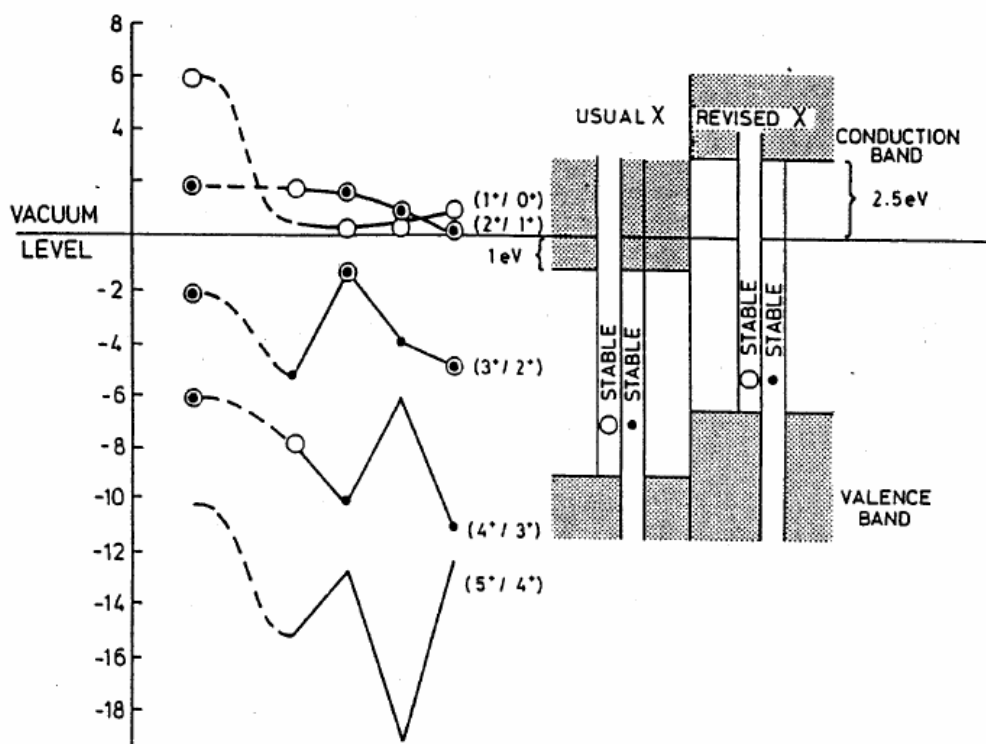


FIG. 2. Energies  $E(N/N + 1)$  for Mn, Fe, Co, and Ni (from left to right) in MgO, calculated by Stoneham et al. (1981). The marked points indicate observed charge states, the different symbols describing the range of stability (○ above valence band maximum, ● below conduction band, ● within gap). At the right the consequences of different host electron affinities are shown. Only for the value of  $-2.5$  eV (conduction band above vacuum) are observed data consistent with predictions.

the potential for the standard hydrogen electrode, and a very approximate empirical theory (Table I).

Table I shows that there is very respectable accord between electron affinities obtained from electrochemistry, from the Butler and Ginley rules, and from observed charge state stability, when all such data are available (strontium and barium titanates and tin dioxide). For MgO, electrochemical data are not available; Butler and Ginley predict a trend from other oxides consistent with the observed charge states, but their estimate does not go far enough to agree with this new class of experiment. Secondary electron emission (27) appears to match the transition metal ion data; the "usual" values from thermionic emission disagree, but refer to surfaces which are normally un-

characterized or perhaps dirty (hence likely to give an upper bound to the crystal electron affinity).

At this point, it is useful to be reminded of the differences in principle between different measures of "electron affinity" and the like. We shall not duplicate van Vechten's excellent review (3), but remark that there is a real need for care in comparing energies obtained from different experiments (e.g., Fowler plots of photoemission, Richardson plots of thermionic emission, contact potentials, low-energy electron diffraction, etc). In our present case, we remark that observing which states of a transition metal ion are stable does not involve any crystal surface, ideal or real. We simply define an energy common to all dopants which allows us to collate observed charge

TABLE I

Electron affinity (eV)	MgO	SrTiO <sub>3</sub>	BaTiO <sub>3</sub>	SnO <sub>2</sub>
Empirical theory (Butler and Ginley)	1.42	3.71	3.60	4.49
Electrochemistry (Butler and Ginley)	not observed	3.8	3.7	4.5
Charge state stability of dopants	-1 to -2.5 (Stoneham and Sangster)	Probably around 3 eV (see text)	Probably close to SrTiO <sub>3</sub>	+2.5 to +5 (Pandey and Stoneham)
"Usual" list values e.g. thermionic emission	+1			
Secondary electron emission (Namba and Murata)	-4			

states quantitatively. The difficult issues re-emerge when this energy is to be related to, say, electrochemical energies. Fortunately, the results appear to be identical to within the accuracy available at present.

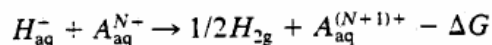
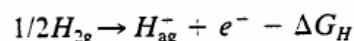
In one class of systems, the crystal affinity problem becomes simpler. This is the case for those nonstoichiometric oxides for which the carriers are small polarons. Essentially, the electron might change a host cation from a 2+ to a 1+ state, and the hole might change a 2+ ion to 3+. This description has been used for ions in uranium (26) to show, for instance, that iodine may be stable in the 1+ charge state at a U site or in the 1- state at the O site when there is excess oxygen, but only at the oxygen site as the 1- charge state otherwise. The dependence on oxygen/uranium ratio arises because an electron released from an impurity will go to a 3+ uranium (self-trapped electron) for stoichiometric or substoichiometric uranium.

#### 4. Further Systems

##### 4.1. Charge State Stability in Aqueous Solution

The choices of reference state and even the sign of the potentials traditionally assigned by electrochemists inevitably lead to confusion of the physicist, despite clear discussions like that of (28). We may, however,

follow some choices directly. Thus (29) define  $\Delta G_H$  and  $\Delta G$  by:



Adding these equations, we find by comparison:

$$E(N/N + 1) = -\Delta G_H + \Delta G$$

Using the value of  $\Delta G_H = 4.48$  eV and the values of  $\Delta G$  listed by Delahay and Dziedzic, we obtain the several values in Table II. These data refer, of course to, thermodynamic equilibrium. The associated optical transitions have thresholds at higher energy. Thus the optical thresholds for the 2+ ions exceed  $E(2/3)$  by 2.59 eV (V), 2.99 eV (Cr) and 2.05 eV (Fe). (28) observes that the reorganization energy (his  $\lambda_r$ , essentially our  $B$ ) is of order 1 eV for many inorganic aqueous redox couples; i.e., much less than the 6 eV discussed earlier for MgO. So, while water has a band gap of 7 eV, similar to MgO, far fewer charge states are stable.

##### 4.2. Surface Reactions with Adsorbed Species

In sensor operation, a gas molecule may be adsorbed on a crystal surface, then change its charge state by transfer of an electron to some site within the crystal. The same processes can occur during the first

TABLE II  
VALUES OF  $E(N/N + 1)$  FOR SOLVATED  
IONS IN WATER

	$E(2/3)$	
Ti	-4.11	(-4.13)
V (0.5 M)	-4.23	(-4.24)
Cr (1 M)	-4.07	(-4.01)
Mn	-6.04	
Fe (1 M)	-5.25	(-5.27)
Ru	-5.34	
	$E(1/2)$	
Ag	-6.48	(-6.46)
Tl	-6.68	
	$E(1/3)$	
Au	-7.18	
	$E(3/4)$	
Ce	-6.08	

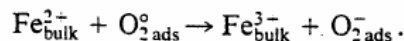
Note. The values are in eV. Note that, for Au, the 2+ state is unstable against disproportionation, so the value quoted does indeed refer to 1+ and 3+. Results are from Delahay and Dziedzic (29), who take  $G_H = 4.48$  eV. Bracketed numbers are from other sources of data.

stages of oxidation too. For the present illustrative example, we shall combine them and, for our own convenience in defining redox energies, we shall regard adsorption as occurring in the ultimate charge state, so that any electron capture or loss by the species to be adsorbed occurs in the gas phase. This is more easily understood from a specific example. Suppose we are interested in  $O_2^-$  on MgO. There are three key energies: the energy  $\varepsilon(O_2^-)$  released on adsorbing  $O_2^-$ ,  $\sim 1.6$  eV; the very small energy  $\varepsilon(O_2^0)$  released on absorbing  $O_2^0$ , and the electron affinity of free  $O_2^0$  (i.e.  $I(0/-1) = 0.44$  eV).

When we consider charge exchange reactions involving  $O_2^0$  and  $O_2^-$ , both adsorbed (so the molecule remains on the surface throughout the process), the redox energy is given by

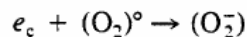
$$E(0/-1) = \varepsilon(O_2^0) - \varepsilon(O_2^-) - I(0/-1).$$

Assuming  $\varepsilon(O_2^0)$  is negligible, and with the estimate  $\varepsilon(O_2^-) \sim 1.6$  eV (this is primarily Coulombic as the anions lie above host cations, (30)) we obtain  $E(0/-1) = -2.04$  eV. Thus, if we consider  $Fe^{2+}$  in bulk MgO (a common impurity), for which  $E(2+/3+)$  is around  $-0.6$  eV, we see that electron transfer to  $O_2^-$  is exothermic:



This type of reaction is typical of one component of gas sensor operation.

A key feature here is the relatively high energy of the electron in the oxide. If we consider  $SnO_2$ , where the bottom of the conduction band is believed below vacuum by about 4 eV, we see the energy cost of the reaction:



is about 3.5 eV. This energy would have to be found from surface processes, whether by chemical reaction, polarization, or as a result of some effect of a surface dipole layer.

#### 4.3. Equilibria Involving Conducting Polymers

For MgO, our working assumption was that the bottom of the conduction band had a well-defined energy, and that our problem was to establish just what it was. The carrier concentrations would always be low too, so interactions between free carriers could be ignored, though clearly experiments exploiting space-charge regions would need more careful treatment (e.g., Hayes and Stoneham, Chap. 7 (18)). This simplicity disappears in several important cases, where the electron affinity changes significantly with carrier number. One example is supported small metal catalyst particles; another which we discuss, is a conducting polymer comprising short chains (perhaps 100 carbons) of various lengths.

Conducting polymers like *trans*-polyacetylene (*t*-PA) introduce new features. Two of the most important are the large relaxation



energies associated with free or bound carriers and the dependence of such energies on chain length, at least for short chains. The most important role of establishing absolute energies is perhaps in understanding carrier injection and the efficiency of electroluminescence. However, other areas of importance include the interpretation of scanning tunnelling microscope images (31, 32). Happily, there are electrochemical data available too (33). For an initial analysis, we shall consider just a single molecule of *t*-PA with  $2n$  carbons. For properties sensitive to  $n$ , we must make an ensemble average over chain lengths before comparison with experiment.

It is especially important here to go beyond the usual one-electron band pictures. What we need is a chemical potential, and specifically what a physicist would identify as the difference between the Fermi level and the vacuum level. This we obtain by self-consistent molecular dynamics, using the Harwell CHEMOS code, which yields the ground state energy  $E(N)$  of the (relaxed) chain with different numbers  $N$  of electrons. This energy is essentially the zero-temperature limit of the Helmholtz free energy. The electron affinity  $A(N)$  (energy gain on adding an electron), and ionization energy  $I(N)$  (energy to remove an electron) can be combined to yield the work function  $W(N)$ , the arithmetic average of  $I(N)$ , and  $A(N)$ .

For many applications, it is useful to have an analytic fit to  $E(N)$ , or better  $E(Q)$  as a function of net charge  $Q$  of the chain. The work function found (32) is then essentially  $W(Q) = [4.67 + 3.9Q]$  eV, and it is this quantity which is needed to establish how much charge will flow when the molecule is (for example) put into contact with a metal electrode. The electrode acts as a reservoir, with Fermi level below the vacuum by an energy equal to the metal work function. Charge flows until the two Fermi levels are equal. Our results can be obtained both by the self-consistent expression for  $W(Q)$  just given, or by the more approximate form us-

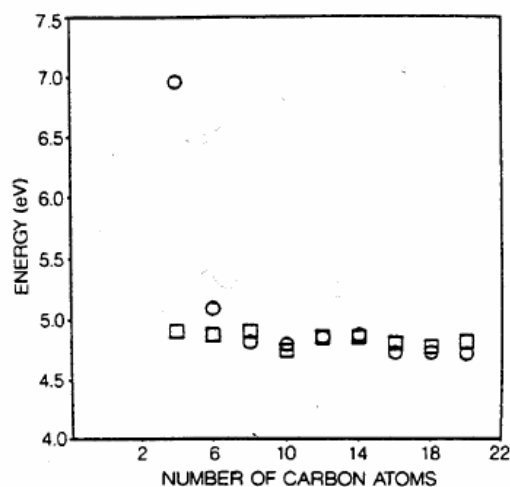


FIG. 3. Variation of the work function of *trans*-polyacetylene ( $t\text{-C}_{2n}\text{H}_{2n-2}$ ) as a function of chain length. The circles are obtained from the electron affinity and ionisation potential calculated explicitly from total energies for different charge states: the squares are obtained from the energies of the highest occupied and lowest unoccupied molecular orbitals. In all cases there was full geometric relaxation and self-consistency. The experimental value (for an unstated chain length) is about 4.6 eV (33).

ing Koopmans theorem, in which the work function is the arithmetic mean of the energies of the highest occupied and lowest unoccupied levels. The two approaches agree very well, and also agree with electrochemical data (Fig. 3).

These results could be used to calculate the equilibrium charge distribution in the presence of transition metal ions, as in the cases discussed above. This is not of great experimental interest, but the predictions do have several implications. First, using the values of  $W(Q)$  with the accepted band gap of 1.7 eV for *t*-PA, we can predict for *p*-type *t*-PA (with Fermi level close to the highest occupied molecular orbitals) that low work-function metals (like Al or In) will form a rectifying junction, whereas high work-function metals (e.g., Au or Pt) should form an ohmic contact. This is reflected in charge transfer at contact. At an Al contact, equilibrium corresponds to about one electron is injected per 10 *t*-PA chains; at an Au con-

tact, about one electron per 10 chains is transferred to the metal. Experiments on organic field effect transistors are consistent with a low density of carriers. Second, we can show that the change in dimerization pattern is very similar to polaron injection. Third, we can go further, and examine the effects of interactions between carriers on two nearby chains. At this stage it is both important (and practical) to include the image interaction of the injected charge with the metal electrode. These two factors (carrier-carrier interactions and image terms) are also important in nonstoichiometric oxides and electrolytes, and hence correspond to common ground between the systems discussed.

## 5. Conclusions

We have addressed some of the issues involved in estimating the electron affinity of ionic solids and understanding which charge state of dopants will be stable. This leads to the surprising (but apparently consistent) conclusion that MgO has a negative electron affinity. Emerging from the analysis too were comparisons with other systems. The definition of electron affinity is by no means so straightforward for conducting polymers. The similarities of observed charge state stability for MgO and, say GaAs, underlie major differences. In the ionic solids it is ionic polarization which stabilizes so many states. For the III-V's it is hybridization and charge transfer. Other systems allow far fewer charge states to be stable. For the rare earths (as opposed to iron group) this is an issue of ionization potential (10, 34). For water (as opposed to MgO) it is the lower reorganization (relaxation) energy which is responsible.

## Acknowledgments

It is a pleasure to dedicate this paper to Professor Sir John Meurig Thomas, FRS. Over the years he has been a major influence in solid-state chemistry, in its

fruitful links with theory, and in its exposition in a way which has encouraged many scientists.

Some of this work was supported by the UKAEA under its Underlying Research Programme, and later its Corporate Research Programme. One of us (MMDR) is indebted to the CEC for support under its Stimulation Programme.

## References

1. P. T. MOSELEY, A. M. STONEHAM, AND D. E. WILLIAMS. "Techniques and Mechanisms in Gas Sensing," p. 108 Adam Hilger, Bristol (1991).
2. A. M. STONEHAM. *Philos. Mag. [Part] B* **51**, 161 (1985).
3. J. H. VAN VECHTEN. *J. Vac. Sci. Technol. B* **3**, 1240 (1985).
4. M. LANNOO AND P. FRIEDEL. "Atomic and Electronic Structure of Surfaces." Springer Series in Surface Science, Vol. 16. Springer Pub., New York (1991).
5. P. W. TASKER. *J. Phys. C* **12**, 4977 (1979).
6. A. M. STONEHAM AND M. J. L. SANGSTER. *Philos. Mag. [Part] B* **43**, 609.
7. A. M. STONEHAM AND M. J. L. SANGSTER. *Radiat. Eff.* **73**, 267 (1983).
8. A. M. STONEHAM, M. J. L. SANGSTER, AND P. W. TASKER. *Philos. Mag. [Part] B* **44**, 603 (1981).
9. J. MENG, J. M. VAIL, A. M. STONEHAM, AND P. JENA. *Phys. Rev. B* **42**, 1156 (1990).
10. A. M. STONEHAM. AEA Report M-3253 (1985).
11. C. R. A. CATLOW AND A. M. STONEHAM. *J. Phys. C* **16**, 4321 (1983).
12. N. F. MOTT AND M. J. LITTLETON. *Trans. Faraday Soc.* **34**, 485 (1938).
13. C. E. MOORE. "Tables of Atomic Energy Levels." NBS No. 467 (1949).
14. K. MIZUSHIMA, M. TANAKA, AND S. IIDA. *J. Phys. Soc. Jpn.* **32**, 1519 (1972).
15. K. MIZUSHIMA, M. TANAKA, A. ASAI, S. IIDA, AND J. GOODENOUGH. *J. Phys. Chem. Solids* **42**, 1129 (1979).
16. R. JAMES. AERE Report TP 814 (1979).
17. C. DELERUE. *Phys. Scr.* **T25**, 128 (1989).
18. W. HAYES AND A. M. STONEHAM. "Defects and Defect Processes in Non-Metallic Solids." Wiley, New York (1985).
19. N. F. MOTT AND R. W. GURNEY. "Electronic Processes in Ionic Solids." Oxford Univ. Press, Oxford (1948).
20. W. D. OHLSEN. *Phys. Rev. B* **7**, 4058 (1973).
21. W. H. ZACHARIESEN. *J. Less-Common Met.* **62**, 1 (1978).
22. K. A. MÜLLER. *J. Phys.* **43**, 551 (1981).
23. M. A. BUTLER AND D. S. GINLEY. *J. Electrochem. Soc.* **125**, 231 (1978).
24. M. A. BUTLER AND D. S. GINLEY. *J. Electrochem. Soc.* **125**, 228 (1978).

25. M. A. BUTLER AND D. S. GINLEY, *Chem. Phys. Lett.* **47**, 319 (1977).
26. R. W. GRIMES, C. R. A. CATLOW, AND A. M. STONEHAM, *J. Amer. Ceram. Soc.* **72**, 1856 (1989).
27. H. NAMBA AND Y. MURATA. ISSP Tech Report 1394 (1983).
28. P. LEMASSON, *J. Cryst. Growth* **72**, 405 (1985).
29. P. DELAHAY AND A. DZIEDZIC. *J. Chem. Phys.* **80**, S793 (1984).
30. A. N. STONEHAM AND P. W. TASKER, unpublished calculations (1985).
31. M. M. D. RAMOS, *J. Phys. Cond. Mat.* **5**, 2483 (1993).
32. M. M. D. RAMOS. Thesis, University of Oxford (1992).
33. A. G. MACDIARMID, R. J. MAMMONE, R. B. KANER, AND S. J. PORTER, *Philos. Trans. R. Soc. Ser. A* **314**, 3 (1985).
34. C. DELERUE AND M. LANNOO, *Mater. Sci. Forum* **83-87**, 659 (1992).